

NEW EXOTIC RARE-EARTH NUCLEI STUDIED WITH A He JET COUPLED  
TO A MASS SEPARATOR ON-LINE WITH SARA

R. BERAUD, A. CHARVET, R. DUFFAUT, A. EMSALLEM, M. MEYER, N. REDON

Institut de Physique Nucléaire (and IN2P3), Université Claude Bernard Lyon-1  
43, Bd au 11 Novembre 1918, F-69622 Villeurbanne Cedex, France

A. GIZON, J. GENEVEY

Institut des Sciences Nucléaires (IN2P3 et USTMG)  
53, Avenue des Martyrs, F-38026 Grenoble Cedex, France

ABSTRACT

Fusion-evaporation reactions with  $^{32}\text{S}$ ,  $^{35}\text{Cl}$  and  $^{36}\text{Ar}$  beams on  $^{92}\text{Mo}$ ,  $^{106}\text{Cd}$  and  $^{112}\text{Sn}$  targets have been used to search for new activities. The reaction products transported via a He-Jet system coupled to a mass-separator for mass identification have been studied by  $\gamma$ -ray and X-ray spectroscopy techniques. Decay schemes of at least seven new isotopes have been derived. Data are presented through systematics and compared to recent theoretical calculations.

1. INTRODUCTION

In the recent past years a great number of interesting results has been gained on the structure of nuclei far off the valley of stability. Recoil spectrometers (BEVALAC, GANIL, ...) have proved their ability in identifying new (proton/neutron)-rich light short-lived isotopes produced in high or intermediate energy H.I. reactions <sup>1,2</sup>. Due to overlapping charge state distributions, the technique unfortunately fails as the mass of the reaction products increases. The standard isotope separator on-line (ISOL), although not so fast, is applicable whatever the mass is and allows decay studies in a very low background environment. The use of high energy proton or  $^3\text{He}$  beams with thick heavy targets at the ISOLDE facility has been probably one of the most powerful tool in producing exotic nuclei <sup>3</sup>. However, the great variety of projectile-target combinations and the kinematical advantage of forward peaking in fusion-evaporation reactions have allowed to discover lot of proton-rich nuclei and new decay modes (p-radioactivity, B-2p, ...) <sup>4,5</sup>.

In this paper I will give a brief description of our He-Jet coupled to a medium current mass separator source and then the results obtained since the facility is in operation.

2. EXPERIMENTAL

2.1 - The accelerator

The experiments have been carried out in Grenoble with the SARA (Système Accélérateur Rhône-Alpes) facility composed of two cyclotrons, a K = 90 compact one and a K = 160 separated sector one. The ECR ion source is now commonly used to get low energy (5-6 MeV(A), high intensity beams ( $> 3 \cdot 10^{11}$  particles/s) with the first cyclotron alone. This configuration was mainly used in the experiments described below, to carry out spectroscopic studies on nuclei produced via fusion-evaporation reactions.

2.2 - The He-Jet fed on-line mass-separator

The layout of the present facility is shown in the schematic plan view of figure 1 and has been described in details very recently <sup>6</sup>. The delay times introduced in classical integrated target-ion sources mainly due to diffusion process of recoils in the catcher material is a severe limitation to the study of short-lived isotopes. The Helium-Jet recoil technique coupled to a mass separator ion source led to a number of successes

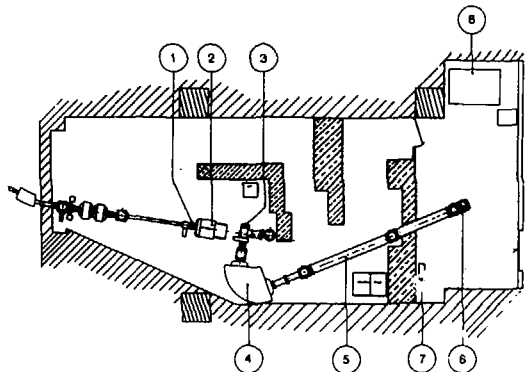


Figure 1 - Layout of the ISOL facility at SARA

- |                           |  |
|---------------------------|--|
| (1) He-jet recoil chamber | (5) Magnet                                     |
| (2) Beam-Stopper          | (6) Tape transport system and counting station |
| (3) Ion-Source            | (7) Tape transport control device              |
| (4) Magnet                | (8) General control desk of separator          |

at the RAMA facility <sup>7</sup>. This method appeared to us very promising in view of studying refractory elements. It is worth to mention two other main advantages :

FR8703286

-- The concept of "cold production" may be applied because the target is located far off the hot environment of the ion source. Therefore, low fusion point and/or high vapour pressure element targets as well as gaseous ones may be used as long they can bear the beam heating.

-- The delay time is roughly equal to the mean transit time in the capillary (~ 1 second for a 10 m long capillary) of the recoils.

I will give a brief description of the original parts of the facility and then the overall performances of the system.

In order to get a fast homogeneous He flow, a sheet-type stopping chamber has been designed and it was found to give better yields than the multicapillary-type chamber for isotopes of a few seconds period.

The stopping chamber (100 mm long and  $\phi = 10$  mm) is placed in the middle of a pressurized (1-2 bars) cube separated from the accelerator vacuum by a 2 mg/cm<sup>2</sup> havar window. The He gas is fed via an aerosol generator and the flow rate continuously controlled with a flow meter (typically 15 cm<sup>3</sup>/s for the 10 m capillary).

A beam stopper composed of successive layers of lead, steel and of boron polystyrene powder is placed behind the reaction cube and protects the experimental area from neutron and  $\gamma$  background induced by the nuclear reactions.

The main part of the system is the integrated skimmer ion-source shown in figure 2 which is composed of a pre-skimmer chamber and a modified version of a Bernas-Nier source. In order to maintain a suitable pressure in the ion-source (~ 5.10<sup>-5</sup> torr) with a skimmer hole, typically 1.2 mm diameter, the pressure in the pre-skimmer region must be

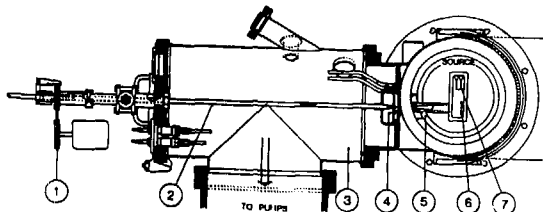


Figure 2 - Plan of the He-Jet injection system

- (1) Remote adjusting system of the distance between capillary end and skimmer
- (2) Rigid pipe holding the capillary
- (3) Pre-skimmer chamber
- (4) Skimmer
- (5) Injection conical canal
- (6) Catcher
- (7) Cathode

lower than 10<sup>-7</sup> Torr and this needs a high flow pumping system composed of two roots and one primary pumps (respectively 3000 m<sup>3</sup>/h - 400 m<sup>3</sup>/h and 120 m<sup>3</sup>/h). The presently improved device with a 8000 m<sup>3</sup>/h roots will allow a significantly higher helium flow in the pre-skimmer chamber.

The separator includes a 120° angle magnet with a mean radius of 0.75 m and n = 1/2 index. The separated beam is transported to the low background counting area by a 6 m long double Einzel lens <sup>18/</sup>.

The detection set-up was designed to perform simultaneously  $\gamma$ - $\gamma$  and X- $\gamma$  coincidences,  $\gamma$ -ray and also delayed particle multianalysis decays for physics experiments. A triangular detection chamber has been designed for that purpose and is presented in figure 3.

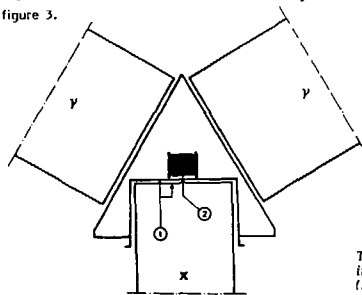


Figure 3

Triangular detection chamber used in X-ray and  $\gamma$ -ray experiments.  
(1) Be windows (2) sample

$\gamma$ -rays have been measured by means of two 40% efficiency intrinsic Ge detectors and X-rays using a small planar one with energy resolution < 450 eV at 122 keV. The experiments were carried out first with the He-jet alone in order to have more  $\gamma$ - $\gamma$  and X- $\gamma$  events allowing decay scheme construction and Z identification. The coupled system was then used only for A identification measuring a simple  $\gamma$  single spectrum.

### 2.3 - Efficiencies of the system

Most of the test experiments have been carried out with the I.P.N. Lyon isotopo separator. They are reported in detail by Olivier <sup>19/</sup>. A great variety of aerosols have been tested with the He-jet angle and in the coupling mode. The best results have been obtained with 1-2 dichloroethane (C<sub>2</sub>H<sub>4</sub>Cl<sub>2</sub>) and are reported in Table 1. Very recently <sup>20/</sup> heated at 400°C has been found to give excellent He-jet transfer yield and led to coupling efficiency of ~ 0.7% for Eu and Sm elements.

It is also worth to mention that chlorination combined to a high catcher temperature allows a substantial yield in lanthanum element versus Ba and Cs. This is shown in figure 4 by the evolution of K $\alpha$  X-rays of Ba, Cs and Xe when varying the source parameters.

Element	Temperature (°C) giving a vapor of $10^{-2}$ Torr for		Yield (at/s) after mass separation	Coupling efficiency (%)
	Element	Chloride		
Barium	610	899	$^{126}\text{Ba}(a)$ $2.0 \cdot 10^2$	0.9
Lanthanum	1727	825	$^{124}\text{La}(a)$ $1.7 \cdot 10^2$	1.7
Eurpium	611	725	$^{138}\text{Eu}(b)$ $2.2 \cdot 10^2$	2.2
Gadolinium	1327	713	$^{141}\text{Gd}(d)$ $1.1 \cdot 10^2$	0.9
			$^{143}\text{Gd}(c)$ $2.0 \cdot 10^2$	
Terbium	1427	< 1000	$^{143}\text{Tb}(c)$ $1.5 \cdot 10^2$	1.1
			$^{147}\text{Tb}(c)$ $3.7 \cdot 10^2$	
Dysprosium	1117	700	$^{140}\text{Dy}(c)$ $2.0 \cdot 10^2$	1.4

**Table 1** - Preliminary production yields and coupling efficiencies obtained at first experiments using the He-jet coupled to the SARA on-line mass-separator in the light rare-earth region. The following nuclear reactions were used:

- (a)  $^{92}\text{Mo} + ^{35}\text{Cl}^{3+}$ , 191 MeV (c)  $^{112}\text{Sn} + ^{35}\text{Cl}^{3+}$ , 191 MeV  
 (b)  $^{108}\text{Cd} + ^{35}\text{Cl}^{3+}$ , 191 MeV (d)  $^{112}\text{Sn} + ^{32}\text{S}^{4+}$ , 168 MeV

The beam intensity was about 100 nAe and the average target thickness was  $2 \text{ mg/cm}^2$ .

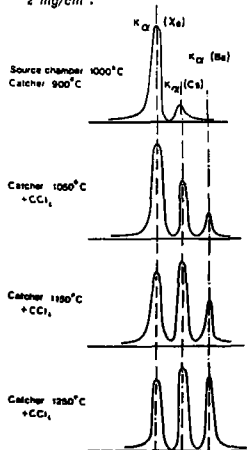


**Figure 4**

Schematic representation of the production of Cs, Ba, La extracted with the He-jet fed mass-separator at  $A = 124$  by using the  $^{92}\text{Mo} + ^{35}\text{Cl}$  reaction at 191 MeV energy. The figure shows the intensities of K $\alpha$  X-rays of Xe, Cs and Ba (accounting respectively for the production of Cs, Ba and La elements) for various source parameters.

### 3. RESULTS

Up to now we have identified seven new neutron-deficient isotopes with  $N < 82$  and  $Z > 50$  and most of their  $\beta$ -decay properties have been recently published [10]. Figure 5 shows the location of these isotopes in the chart of nuclides. They belong to a region close to the proton drip-line where Leander and Möller [11] have predicted the onset of large deformations. More recently self-consistent studies of triaxial deformations have been performed [12] on heavy nuclei, establishing the triaxial stability of the intrinsic state of  $^{138}\text{Sm}$ .

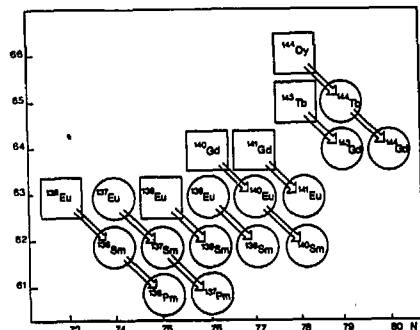


**Figure 5** - Part of the nuclear chart related to the mass region investigated.

In this paper I will mainly emphasize the new experimental results and try to extract some structural effects by analysing the evolution of low-lying energy levels along particular systematics.

#### 3.1 - The Eu-Sm region

In a very recent experiment, 234 MeV  $^{36}\text{Ar}$  beam has been used to bombard a  $2 \text{ mg/cm}^2$  enriched  $^{106}\text{Cd}$  target. Using the set-up described in section 2.2, a set of measurements including  $\gamma$ -ray multianalysis ( $16 \times 0.5$  s), X- $\gamma$  ray and  $\gamma$ - $\gamma$  coincidences were performed. Two  $\gamma$ -rays (255.0 keV and 431.5 keV) with a half-life of  $(3.7 \pm 0.5)\text{s}$  were found to be coincident with K $\alpha$  X-rays of Sm. As they are present in the mass separated  $\gamma$  spectrum at mass  $A = 136$ , this allows to propose in figure 6 a preliminary decay scheme for  $^{136}\text{Eu} + \text{Sm}$ . Figure 7 shows the decay pattern of the two lines involved and figure 8 exhibits a  $\gamma$  spectrum coincident with Sm K $\alpha$  X-rays. These results are corroborated by recent in-beam experiments on  $^{136}\text{Sm}$  [13,14].

In the even-even isotopes of Nd and Cd with  $N < 82$  the energy of the first excited  $2^+$  state, which roughly characterises the nuclear quadrupole deformation, goes down

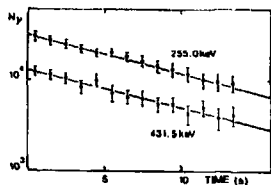


Figure 7 - ( $16 \times 0.5$  s) decay of the 255.0 keV and 431.5 keV  $\gamma$  transitions ascribed to  $^{136}\text{Eu} \rightarrow \text{Sm}$  decay.

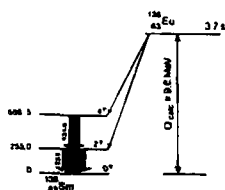


Figure 6 - Preliminary decay scheme of 3.7 s  $^{136}\text{Eu}$ .

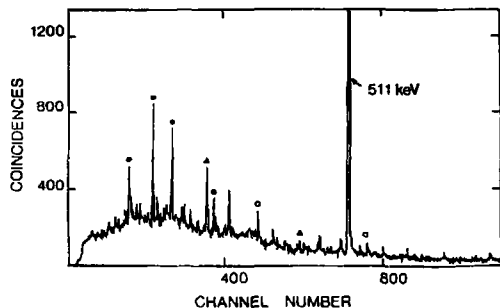


Figure 8 -  $\gamma$ -ray spectrum coincident with Sm  $K\alpha$  X-rays in the  $^{36}\text{Ar} + ^{106}\text{Cd}$  reactions. (•)  $^{139}\text{Eu} \rightarrow \text{Sm}$ ; (◦)  $^{138}\text{Eu} \rightarrow \text{Sm}$ ; (▲)  $^{136}\text{Eu} \rightarrow \text{Sm}$

smoothly when  $N$  decreases. From figure 9 it is obvious that the Sm isotopes seem to follow a similar trend and the energy ratio ( $4.3/2.7$ ) reflects also the onset of an increasing deformation. The value of this ratio for  $^{136}\text{Sm}$  and  $^{138}\text{Sm}$  is around 2.6 indicating a possible  $\gamma$  asymmetry.

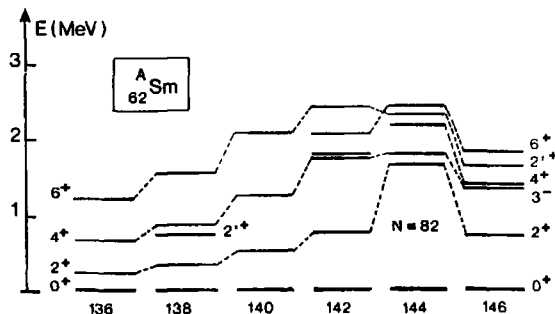


Figure 9 - Systematics of the first excited states in  $^{136-146}\text{Sm}$ . Both data from in-beam and decay studies have been used.

The existence in  $^{138}\text{Sm}$ ,  $^{138}\text{Nd}$  and  $^{136}\text{Nd}$  of a second  $2^+$  below the first excited  $4^+$  level and the fact that the sum of the energies of the two first  $2^+$  levels is equal within a few percent to the first  $3^+$  level energy are characteristic features of a rotating triaxial nucleus <sup>151</sup>. This phenomenon predicted by Ragnarsson et al. <sup>161</sup> for  $N = 76$  isotones is strongly suggested by the bunching of the levels  $13/2^+$ ,  $15/2^+$  and  $17/2^+$ ,  $19/2^+$  for  $N = 77$  isotopes of odd Nd and Ce.

As the nuclear shape depends strongly on the shell corrections, microscopic calculations are appropriate to describe the properties of these isotopes. Constrained Hartree-Fock + BCS triaxial calculations <sup>172</sup> have been recently performed with an effective nucleon-nucleon force of the Skyrme type (S III) and have confirmed a stable triaxial deformation for the intrinsic state of  $^{138}\text{Sm}$ . From the minimum of energy in the deformation energy surface we can extract an asymmetry angle  $\gamma = 25^\circ$  and a mass quadrupole moment of  $0.45 \text{ fm}^2$  which is compatible with a  $\beta_2 = 0.2$ .

### 3.2 - The $126\text{-Ba}$ region

In comparison with the neighbouring region which has been extensively studied by both in-beam  $\gamma$ -ray spectroscopy and radioactive decay experiments, the barium isotopes are less known due to the difficulties in producing short-lived isotopically separated lanthanum samples.

For even Ba isotopes and odd ones as well, many high spin states are known [17,18,19] up to  $6-7$  MeV excitation energy but very scarce results are available on the low-energy levels of these isotopes.

Therefore, using various F.L. fusion reactions as  $^{35}\text{Cl} + ^{92,94,96}\text{Mo}$  and  $^{36}\text{Ar} + ^{92,96}\text{Mo}$ , we have collected  $^{124,124}, ^{125}, ^{126}\text{La}$  separated samples with the facility described in section 2. I will report here partial results deduced from these measurements for both  $^{126}\text{Ba}$  and  $^{124}\text{Ba}$ .

#### 3.2.1 - $^{126}\text{La} + ^{126}\text{Ba}$ decay

The  $^{126}\text{Ba}$  level scheme, presented in figure 10(a), was established from  $\beta$ -decay of  $^{126}\text{La}$ . It contains the first members of the g.s. band, the quasi-gamma band and three negative parity states in good agreement with in-beam results [18,19].

Two new levels at 983.5 and 1296 keV excitation energy are well established by  $\gamma$ - $\gamma$  coincidences. Because of their energies and deexcitation modes, tentative ( $0^+$ ) and ( $2^+$ ) labels are proposed. Obviously, conversion electron measurements are needed to confirm these assignments. The existence of two isomers in  $^{126}\text{La}$  seems very probable: one of medium spin ( $l = 5$  or  $6$ ) and one of low-spin ( $l = 1$  or  $2$ ) feeding directly the new ( $0^+$ ), ( $2^+$ ) sequence. From our decay measurements only one half-life  $T_{1/2} = (64 \pm 3)$  seconds was found and this remains an open problem.

#### 3.2.2 - $^{124}\text{La} + ^{124}\text{Ba}$ decay

In figure 10(b) is presented the  $^{124}\text{Ba}$  level scheme established from  $\beta$ -decay of  $^{124}\text{La}$ . Spin and parity assignments have been made on the basis of analogy with heavier e-e barium.  $^{120}\text{Ba}$  and  $^{126}\text{Ba}$  level scheme exhibit striking similarities excepting the feeding of  $B^+$  levels in  $^{124}\text{Ba}$  which is possible because of a probable 7 or 8 spin for the high-spin isomer of  $^{124}\text{La}$ .

A new sequence including levels at 1927( $1^+$ ), 1211( $2^+$ ) and 1672( $4^+$ ) has been established, suggesting another decay path from a low-spin  $^{124}\text{La}$  ( $l = 3$  or  $4$ ).

Unfortunately, no new half-life has been observed in addition to the well-known ( $29 \pm 2$ ) seconds [20,21] period.

Different approaches may be applied to interpret the structure of the e-e Ba isotopes:

- The interacting boson model has given a rather good agreement between calculated and experimental g.s. and quasi-gamma bands [22].
- Microscopic calculations [12,23] which take into account the shell corrections would be probably more realistic to explain the shape coexistence suggested by the collective bands ( $11/2^-$  and  $7/2^-$ ) observed in odd-A barium.

Figure 10(a)

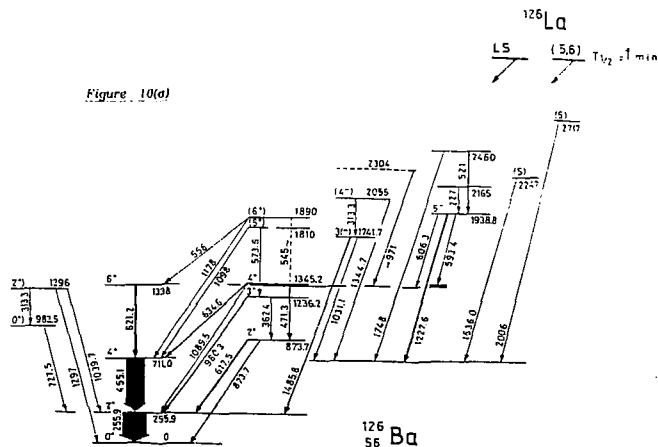
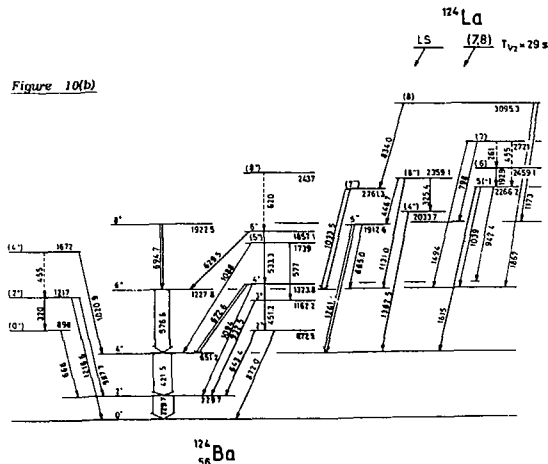


Figure 10(b)



## CONCLUSION

Both experimental and theoretical results have shown the onset of  $\gamma$  asymmetry near  $N = 76$  and it would be highly desirable to follow this shape transition via :

- i) the study of high spin excited states ( $11/2$  band) in odd samarium isotopes with in beam experiments,
- ii) decay studies in order to locate the " $\gamma$  band" in e-e isotopes,
- iii) particle spectroscopy and  $D_2$  measurements for the most neutron deficient ones which would give experimental masses.

## ACKNOWLEDGMENTS

The authors wish to thank V. Boninchi, G. Margotton, J.P. Richard, S. Vanzetto, L. Vidal, J.L. Vieux-Rochaz and especially A. Plantier for valuable technical assistance in carrying out the experiments. We are also indebted to the SARA staff, J. Aystö, J. Honkanen (University of Jyväskylä) and K. Deneffe (I.K.S. Leuven) are greatly acknowledged for their collaboration.

## References

- 1 M.J. Murphy et al., Phys. Rev. Lett., 1982, 49, 455
- 2 C. Detraz, This Conference and  
D. Guerreau, J. de Phys., Coll. C-4, 1986, 47, 207
- 3 H. Ravn, EMIS-11 Los Alamos, August 1986  
(to be published in "Nucl. Instr. and Meth. in Phys. Res.")
- 4 E. Roeckl, Nucl. Phys., 1983, A-400, 131c
- 5 J. Aystö et al., Phys. Rev. Lett., 1985, 55, 1384
- 6 A. Plantier et al., EMIS-11 Los Alamos, August 1986  
(to be published in "Nucl. Instr. Meth. and Meth. in Phys. Res.")
- 7 D.M. Moltz et al., Nucl. Instr. Meth., 1980, 172, 519
- 8 N. Idrissi, J.P. Belmont, ISN Grenoble-Report, 1986
- 9 T. Ollivier, Doct. Thesis, Lyon-1 Univ., 1986
- 10 N. Redon et al., Z. Phys., 1986, A-325, (in press)
- 11 G.A. Lüscher, P. Möller, Phys. Lett., 1982, 110-B, 17
- 12 N. Redon et al., Phys. Lett., (in press)
- 13 C.J. Lister et al., Phys. Rev. Lett., 1985, 55, 810
- 14 A. Makishima et al., Phys. Rev., 1986, C-34, 576
- 15 A.S. Davydov, G.F. Filippov, Nucl. Phys., 1958, B, 237
- 16 I. Ragnarsson et al., Nucl. Phys., 1974, A-233, 329
- 17 J. Gizon et al., Nucl. Phys., 1977, A-277, 464
- 18 C. Fraun et al., Phys. Rev. Lett., 1974, 33, 973
- 19 K. Schaffer et al., Zeit. für Phys., 1986, A-523, 487
- 20 D.D. Bogdanov et al., Nucl. Phys., 1978, A-307, 421
- 21 T. Tamura et al., Nucl. Data Sheets, 1984, 41, 413
- 22 G. Puddu et al., Nucl. Phys., 1980, A-340, 109
- 23 K.W. Schmid et al., Nucl. Phys., 1984, A-431, 205